Development and characterization of 3-(benzylsulfonamido)benzamides as potent and selective SIRT2 inhibitors

ARTICLE · JANUARY 2014

CITATIONS
3

READS
44

6 AUTHORS, INCLUDING:

Aleksey Kazantsev
Massachusetts General Hospital
77 PUBLICATIONS **6,397** CITATIONS
SEE PROFILE

Richard B. Silverman
Northwestern University
327 PUBLICATIONS **5,839** CITATIONS
SEE PROFILE

European Journal of Medicinal Chemistry 76 (2014) 414–426

Contents lists available at ScienceDirect

European Journal of Medicinal Chemistry

journal homepage: http://www.elsevier.com/locate/ejmech

Original article

Development and characterization of 3-(benzylsulfonamido) benzamides as potent and selective SIRT2 inhibitors

Mohammad A. Khanfar [a,b], Luisa Quinti [c], Hua Wang [a], Soo Hyuk Choi [a,1], Aleksey G. Kazantsev [c,**], Richard B. Silverman [a,*]

[a] Department of Chemistry, Department of Molecular Biosciences, Chemistry of Life Processes Institute, Center for Molecular Innovation and Drug Discovery, Northwestern University, 2145 Sheridan Road, Evanston, IL 60208-3113, USA
[b] Department of Pharmaceutical Sciences, The University of Jordan, Amman, Jordan
[c] Department of Neurology, Harvard Medical School and Massachusetts General Hospital, Charlestown, MA 02129-4404, USA

ARTICLE INFO

Article history:
Received 31 October 2013
Received in revised form
23 January 2014
Accepted 5 February 2014
Available online 6 February 2014

Keywords:
SIRT2
Huntington's disease
3-(Benzylsulfonamido)benzamides
Polyglutamine aggregation
ADME

ABSTRACT

Inhibitors of sirtuin-2 deacetylase (SIRT2) have been shown to be protective in various models of Huntington's disease (HD) by decreasing polyglutamine aggregation, a hallmark of HD pathology. The present study was directed at optimizing the potency of SIRT2 inhibitors containing the neuroprotective sulfobenzoic acid scaffold and improving their pharmacology. To achieve that goal, 176 analogues were designed, synthesized, and tested in deacetylation assays against the activities of major human sirtuins SIRT1-3. This screen yielded 15 compounds with enhanced potency for SIRT2 inhibition and 11 compounds having SIRT2 inhibition equal to reference compound AK-1. The newly synthesized compounds also demonstrated higher SIRT2 selectivity over SIRT1 and SIRT3. These candidates were subjected to a dose–response bioactivity assay, measuring an increase in α-tubulin K40 acetylation in two neuronal cell lines, which yielded five compounds bioactive in both cell lines and eight compounds bioactive in at least one of the cell lines tested. These bioactive compounds were subsequently tested in a tertiary polyglutamine aggregation assay, which identified five inhibitors. ADME properties of the bioactive SIRT2 inhibitors were assessed, which revealed a significant improvement of the pharmacological properties of the new entities, reaching closer to the goal of a clinically-viable candidate.

1. Introduction

Sirtuin 2 (SIRT2) deacetylase belongs to class III of histone deacetylases (HDAC); unlike classes I and II, class III HDAC enzyme activities are strictly dependent on a NAD^+ cofactor [1]. Known substrates of SIRT2 deacetylase include diverse cellular proteins, α-tubulin [2], the major component of microtubules, histones 3 and 4, transcription factors FOXO1 and FOXO3a, and many others [3]. SIRT2 is ubiquitously expressed in all tissues and most abundant in the central nervous system. SIRT2 expression levels are dramatically increased during neurodevelopment and remain strikingly high in the adult brain [2]. Pharmacological inhibition of SIRT2 increases neuronal survival in animal models of Parkinson's disease (PD), which is associated with changes in protein inclusion body characteristics [4]. In addition, SIRT2 inhibition by genetic and pharmacological means mediates protection in neuronal and invertebrate models of Huntington's disease (HD), which is also associated with a reduction in polyglutamine aggregates, a hallmark of HD pathology [5].

SIRT2 has also been suggested to play a role in tumorigenesis through its inhibitory effects on p53 [6]. Recent studies have provided strong evidence that the biological function of SIRT2 can be linked to glioma tumourigenesis [7]. SIRT2 functions to release mitotic arrest in critically damaged cells, allowing them to proceed to apoptosis [8,9].

Several diverse SIRT2 inhibitors were discovered in the last few years, including but not limited to, evodiamine alkaloids [10], pseudopeptidic [11], 1,8-dioxodecahydroacridines [12], thieno[3,2-

Abbreviations: CNS, central nervous system; HD, Huntington's disease; HDAC, histone deacetylase; SIRT2, sirtuin-2; PolyQ, polyglutamine.

* Corresponding author.
** Corresponding author. Department of Neurology, Harvard Medical School and Massachusetts General Hospital, Building 114-3300, 16th Street, Charlestown, MA 02129-4404, USA.
E-mail addresses: akazantsev@mgh.harvard.edu (A.G. Kazantsev), Agman@chem.northwestern.edu, r-silverman@northwestern.edu (R.B. Silverman).
[1] Current address: Department of Chemistry, Yonsei University, Seoul, Republic of Korea.

http://dx.doi.org/10.1016/j.ejmech.2014.02.003
0223-5234/

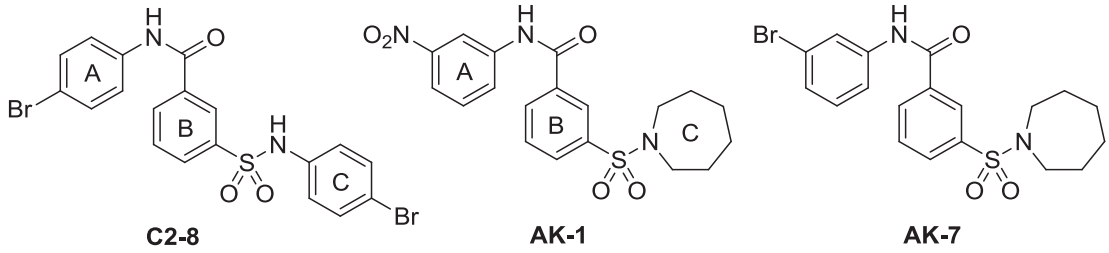

Fig. 1. Structures of neuroprotective polyglutamine aggregation inhibitors: sulfobenzoic acid derivatives **C2-8**, **AK-1**, and **AK-7**.

d]pyrimidine-6-carboxamides [13], salermide analogues [14], carprofen analogues [15], benzodeazaoxaflavins [16], chromone/chroman-4-one [17], anilinobenzamides [18], splitomicin analogues [19], and oxadiazole-carbonylaminothioureas derivatives [20]. The sulfobenzoic acid derivatives described here add to this list of active SIRT2 inhibitor scaffolds.

Efficacy of the sulfobenzoic acid derivative SIRT2 inhibitor, **AK-1** (SIRT2 IC_{50} = 12.5 μM), in PD and HD models has been described (Fig. 1) [4,5,21]. Brain permeability of its close structural analogue, the selective SIRT2 inhibitor **AK-7** (IC_{50} = 15.5 μM), has been reported [21]. In recent studies we have shown that treatment with **AK-7** improved motor function, extended survival, reduced brain atrophy, and was associated with marked reduction of aggregated mutant huntingtin in two genetic mouse models of HD [22]. Brain permeability of sulfobenzoic acid derivative **C2-8**, which is neuroprotective in HD mice, was identified in a phenotypic aggregation screen and has been reported; this structural scaffold also has been used to develop potent and selective SIRT2 inhibitors (Fig. 1) [21,23,24].

Compelling efficacy data associated with sulfobenzoic acid derivatives in diverse models of neurodegeneration suggest further investigation of this structural class as SIRT2 inhibitors for preclinical drug development. Extensive structure modification of lead compounds **AK-7** and **C2-8** has resulted in a variety of analogues with improved SIRT2 inhibition potency and pharmacological properties.

2. Results and discussion

2.1. Chemistry

Syntheses of 3-sulfonamide benzoate derivatives began from commercially available benzoic acid or 4-methoxybenzoic acid (**1**,**2**) using procedures described in the literature (Scheme 1) [25]. The

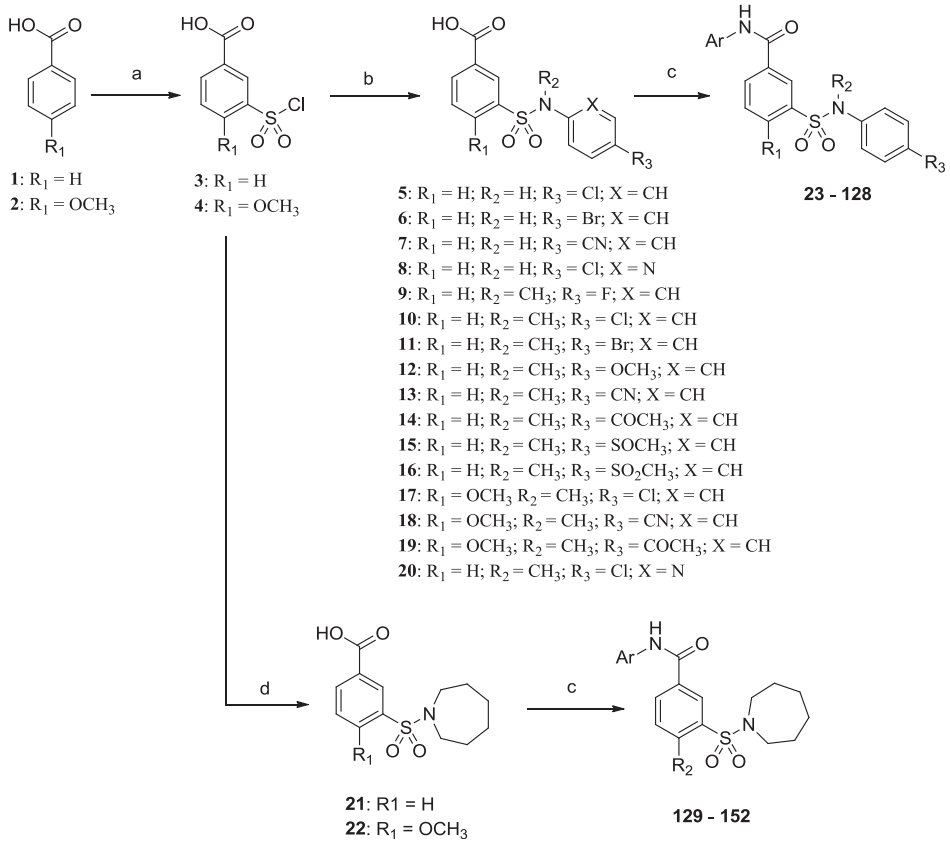

Scheme 1. General synthetic routes to new analogues of **C2-8**, **AK-1**, and **AK-7**. Reagents and conditions: (a) $ClSO_3H$, 65 °C; (b) aniline, pyridine, EtOAc; (c) Ar–NH_2, EDCI, DMAP, CH_2Cl_2; 12 h; (d) azepane, pyridine, EtOAc.

synthetic route started with sulfonylation of **1** and **2** to produce **3** and **4**, respectively, which were coupled with primary or secondary anilines (to give **5**–**20**) or with azepane (to give **21** and **22**) in pyridine to generate the corresponding sulfonamide derivatives. The carboxylic acid was then coupled with the aniline or other heterocyclic rings using *N*-ethyl-*N*′-(3-dimethylaminopropyl)carbodiimide hydrochloride (EDCI) and 4-(dimethylamino)pyridine (DMAP) to generate the final compounds (**23**–**152**; Supporting Information Tables S1 and S2). DMAP was removed in the last step of the syntheses of **23**–**42** to overcome polymerization that has been observed. The commercially available aminothioanisole derivatives (**153** and **154**) were used to synthesize the corresponding sulfoxides (**155** and **156**), using self-catalyzed selective oxidation [26], and sulfones (**157** and **158**), using sodium tungstate and an excess of hydrogen peroxide [27] (Scheme S1 in the Supporting Information).

N-Methyl-4-(methylthio)aniline (**161**) and 5-chloro-*N*-methylpyridin-2-amine (**162**) were synthesized from the corresponding commercially available demethylated derivatives (**154** and **160**, respectively) using the Chan-Lam selective monomethylation procedure, which involves copper(II)-promoted coupling of anilines and methyl boronic acid [28] (Scheme S2 in the Supporting Information). Subsequently, **161** was oxidized to the sulfoxide (**163**) and sulfone (**164**) intermediates, as described above.

The phenolic analogues (**35**, **58**, **70**, **84**, **152**; Tables S1 and S2) were generated from their parent anisole compounds (**29**, **55**, **69**, **83**, **151**, respectively) using one molarity of boron tribromide (BBr_3) in DCM, as described in the literature [29]. Reduction of the acetyl group of **103**, **104**, and **107** was performed using sodium borohydride ($NaBH_4$) in anhydrous methanol [30] to generate secondary alcohol derivatives **126**, **127**, and **128** (Table S1), respectively.

2-Sulfonamide isonicotinamide derivatives **169** and **170** were synthesized from commercially available methyl 2-chloroisonicotinate, as described in Scheme 2. Heating of a suspension of methyl 2-chloroisonicotinate and NaSH in EtOH to 150 °C in a sealed tube generated the corresponding thiol derivative [31]; chlorosulfonyl derivative **168**, generated by NaClO oxidation, was coupled later with suitable anilines to synthesize the corresponding 2-sulfonamide isonicotinamide derivatives (**169** and **170**).

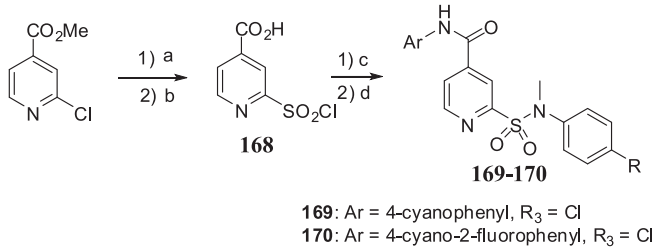

Scheme 2. Synthetic route to 2-sulfonamide isonicotinamide derivatives. Reagents and conditions: (a) NaSH, EtOH, 150 °C sealed tube, 12 h, H_2O; yield 99%; (b) NaClO, HCl (conc.) 0 °C, 2 h; (c) *N*-Methylaniline, pyridine, EtOAc, 6 h; (d) Ar–NH_2, EDCI, DMAP, CH_2Cl_2, 12 h.

The inverse amide linker analogues (**175**, **176**) were synthesized as described in Scheme 3. Starting from commercially available 3-nitrophenylsulfonyl chloride, the sulfonamides were generated from nucleophilic attack by the corresponding *N*-methylanilines in EtOAc and pyridine at room temperature followed by Pd/C catalyzed hydrogenation and EDCI/DMAP coupling to produce compounds **175** and **176**. The synthetic derivatives are summarized in Tables S1– S3 in the Supporting Information.

2.2. Activity of synthetic analogues with SIRT1, SIRT2, and SIRT3

To evaluate the potency and selectivity of the synthesized compounds we employed robust, sensitive, and quantitative biochemical sirtuin deacetylation assays (SIRT1, 2, 3), as previously described [4]. Compounds were screened at a single 10 μM dose in triplicate in the primary SIRT2 assay and counter-screened in SIRT1 and SIRT3 assays. **AK-1** was included as the most potent reference compound with each assay. Hits demonstrating higher or equal potency to that of **AK-1** for SIRT2 inhibition were selected for dose–response studies, which were performed in multiple doses in the primary SIRT2 assay, including **AK-1** for direct comparison. These compounds also were subjected to SIRT1 and SIRT3 assays in multiple doses to determine sirtuin selectivity (Tables S4 and S5 in the Supporting Information). The dose–response assays identified **47**, **54**, **61**, **64**, **90**, **102**, **106**, **115**, **124**, **126**, **165**, **166**, **167**, **169**, and **176** as being more potent SIRT2 inhibitors than **AK-1** (Table 1). SIRT2 activity dose–response profiles for five of the best inhibitors are shown in Fig. 2. Several analogues, **51**, **52**, **57**, **59**, **71**, **103**, **109**, **117**, 170, and **175** had potencies comparable to **AK-1** (Table 2). However, all modifications made on the **AK-1** scaffold failed to improve the SIRT2 inhibitory activity greater than that of **AK-1** (Table S2 in the Supporting Information).

The most potent SIRT2 inhibitors showed a high degree of selectivity; most of the compounds were inactive in SIRT1 and SIRT3 inhibitory assays. Compounds **47**, **61**, **90**, **106**, **124**, **169**, and **170** showed SIRT1 and SIRT3 inhibition lower than 25% when tested at multiple doses up to a concentration of 50 μM; compound **126** showed 29% SIRT1 and SIRT3 inhibition at 25 μM concentration (Tables S5 and S6 in the Supporting Information).

Our compounds showed comparable low micromolar potency and SIRT2-selectivity for two scaffolds of SIRT2 inhibitors that were recently designed, the 2-anilinobenzamide analogues [18] and chromone/chroman-4-one derivatives [17]. The most potent compounds in the 2-anilinobenzamide and chroman-4-one groups have IC_{50} values of 0.57 μM and 1.5 μM, respectively.

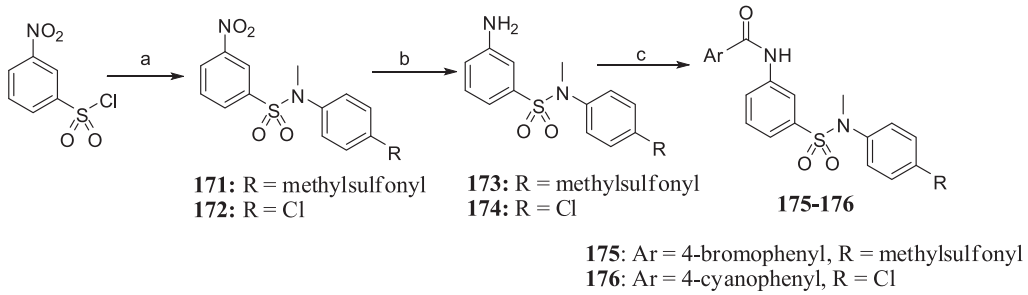

Scheme 3. Synthetic routes to the inverse amide linker analogues. Reagents and conditions: (a) *N*-Methylanilines, pyridine, EtOAc, 6 h; (b) Pd/C (10%), H_2, MeOH/ethyl acetate (1:1) 12 h; (c) Ar–CO_2H, EDCI, DMAP, CH_2Cl_2, 12 h.

Table 1
Novel SIRT2 inhibitors more potent than **AK-1**.

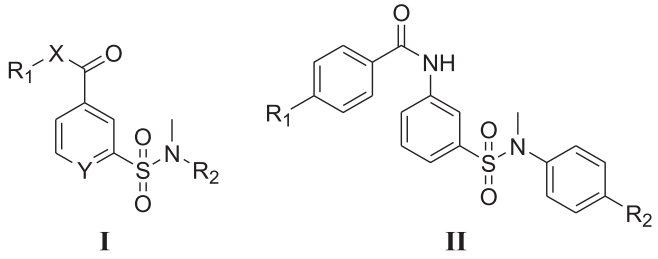

Cmpd no.	Scaffold	R_1	R_2	X	Y	SIRT2 IC_{50} (μM)	% SIRT1 inhibition at 10 μM	% SIRT3 inhibition at 10 μM
AK-1	–	–	–	–	–	**10.8**	10	5
47	I	4-Cyanophenyl	4-Fluorophenyl	NH	CH	**9.4**	11	2
54	I	2-(5-Fluoropyridine)	4-Chlorophenyl	NH	CH	**9.1**	0	0
59	I	4-(Methylsulfinyl)phenyl	4-Chlorophenyl	NH	CH	**9.5**	0	6
61	I	4-(Methylsulfonyl)phenyl	4-Chlorophanyl	NH	CH	**9.8**	3	10
64	I	4-Cyanophenyl	4-Chlorophenyl	NH	CH	**6.1**	5	0
90	I	4-Cyanophenyl	4-Methoxyphenyl	NH	CH	**9.6**	4	6
102	I	4-Chlorophenyl	4-Acetophenyl	NH	CH	**6.8**	0	7
106	I	4-Cyanophenyl	4-Acetophenyl	NH	CH	**7.3**	5	5
115	I	4-Cyanophenyl	4-(Methylsulfonyl)phenyl	NH	CH	**9.5**	9	0
124	I	4-Cyanophenyl	2-(5-Chloropyridine)	NH	CH	**6.1**	10	8
165	I	4-Chloro-2-fluorophenyl	4-Bromophenyl	NCH_3	CH	**7.5**	4	3
166	I	4-Bromo-2-fluorophenyl	4-Bromophenyl	NCH_3	CH	**6.9**	0	0
167	I	4-Cyano-2-fluorophenyl	4-Bromophenyl	NH	CH	**6.6**	9	0
169	I	4-Cyanophenyl	4-Chlorophenyl	NH	N	**4.9**	9	2
175	II	Br	SO_2CH_3	–	–	**6.3**	14	13
176	II	CN	Cl	–	–	**3.8**	20	16

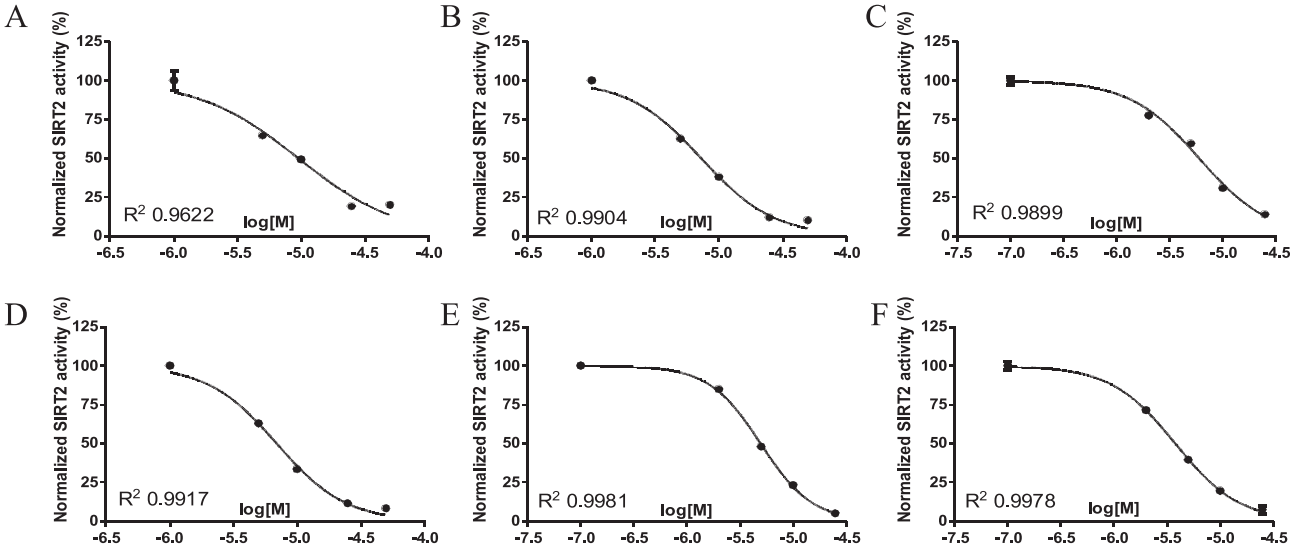

Fig. 2. SIRT2 inhibition dose response curves for six of the most potent compounds. A, **90**; B, **106**; C, **124**; D, **166**; E, **169**; F, **176**. R^2 values for the IC_{50} curve fittings are indicated.

The dose–response curves of captured hits exhibit Hill slope values between −1 and −2, excellent correlation coefficients, and low standard errors (Table S6 in the Supporting Information), which strongly suggest the authenticity (i.e., non-promiscuity) of the SIRT2 inhibitors and support the derived SAR described below.

2.3. Activity of SIRT2 inhibitors in a secondary cell-based acetylation assay

To assess SIRT2 inhibition activity in live cells, we measured an increase in α-tubulin K40 acetylation, a known substrate for SIRT2 deacetylase, in neuronal rat ST14A and mouse Neuro2a cell lines. In this bioactivity test, extracts from cells treated with compounds for 6 h at a range of concentrations were resolved on SDS-PAGE and subjected to Western blot analysis using a primary antibody specific to acetylated lysine-40 of α-tubulin.

Twenty five newly synthesized SIRT2 inhibitors were tested, and five of them, **47**, **90**, **102**, **106**, and **124**, increased α-tubulin acetylation in a dose-dependent manner in both cell lines. Fig. 3 shows the bioactivity of SIRT2 inhibitors **90**, **106**, and **124**, respectively, after 6 h treatment in ST14A cells at concentrations ranging from 0.5 to 50 μM. Compounds **59**, **64**, **109**, **126**, **165**, **166**, **170**, and **175**

Table 2
Novel SIRT2 inhibitors having potencies comparable to that of **AK-1**.

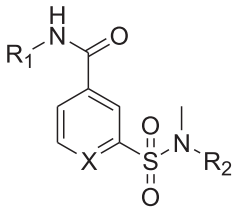

I

Cmpd no.	Scaffold	R_1	R_2	X	SIRT2 IC_{50} (μM)	% SIRT1 inhibition at 10 μM	% SIRT3 inhibition at 10 μM
AK-1	–	–	–	–	**10.8**	10	5
51	I	3-(6-Chloropyridazine)	4-Chlorophenyl	CH	**15.6**	6	0
52	I	2-(5-Chloropyrimidine)	4-Chlorophenyl	CH	**16.1**	0	4
71	I	2-(5-Cyanopyridine)	4-Chlorophanyl	CH	**19.9**	13	N.D.
103	I	2-(5-Chloropyridine)	4-Acetophenyl	CH	**13.2**	11	0
109	I	4-acetophenyl	4-Acetophenyl	CH	**18.9**	5	0
117	I	4-Chlorophenyl	4-(Methylsulfonyl)phenyl	CH	**15.9**	0	0
126	I	4-Cyanophenyl	4-(1-Hydroxyethyl)phenyl	CH	**11.5**	17	9
170	I	4-Cyano-2-fluorophenyl	4-chlorophenyl	N	**10.2**	6	4

increased acetylation of α-tubulin in at least one of the two neuronal cell lines in which they were tested. Compound **90** was found to be the most bioactive in this assay despite not having the highest SIRT2 inhibition activity *in vitro*. A comparison of compounds **90** and **106** in Neuro2a cells is shown in Fig. 3B, C.

During compound treatment in cells, the toxicity of the compounds was monitored. Most of the SIRT2 inhibitors were nontoxic up to 50 μM during a 6 h treatment. Compound **90** was found to be partially toxic at 25 and 50 μM in Neuro2a cells; however, no toxicity was observed in ST14A cells up to an 18 h treatment.

2.4. Activity of SIRT2 inhibitors in a tertiary aggregation assay

The most promising bioactive SIRT2 inhibitors were tested in a previously established polyglutamine aggregation assay using rat neuronal PC12 cells expressing a short fragment of mutant huntingtin in an inducible fashion [32,33]. The effects of these bioactive SIRT2 inhibitors on polyglutamine aggregation were first examined visually by fluorescence microscopy and then assessed by the dot-blot assay in an initial assessment at a dose of 25 μM and repeated at 10 and 25 μM doses (Fig. 4). Expression of the mutant huntingtin fragment was induced in PC12 cells simultaneously to compound treatment with 2.5 μM concentration of inducer muristerone A for 24 h, which resulted in the formation of polyglutamine aggregates, visible in cells as large fluorescent inclusion bodies (Fig. 4A). Inhibition of aggregation in this cell model can be detected as a reduction in the number and size of fluorescent polyglutamine inclusions (Fig. 4B).

To detect the inhibition of polyglutamine aggregates by an independent measurement, we employed a modified filter-trap

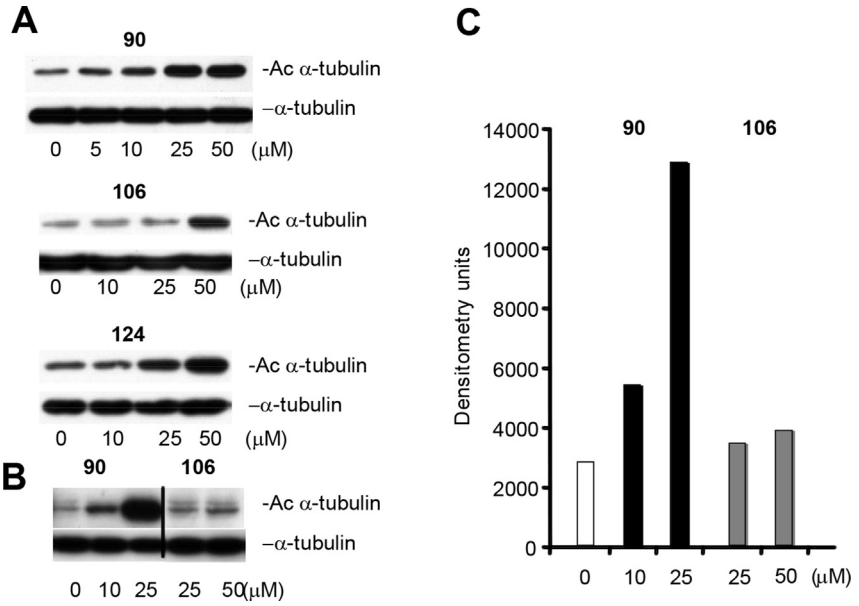

Fig. 3. SIRT2 inhibitor effects on acetylation of α-tubulin K40. A) Treatment of ST14A striatal cells with compounds **90**, **106**, and **124** for 6 h resulted in an increase of α-tubulin acetylation as detected by immunoblotting; α-tubulin is shown as a loading control. B) Direct comparison of compounds **90** and **106** on the increase of α-tubulin acetylation in the neuronal cell line Neuro2a. C) Compound dose-dependent increase of α-tubulin acetylation, normalized to α-tubulin levels, and quantified from Western blots in B). 0 μM concentration is shown in white; it is the baseline for the assay.

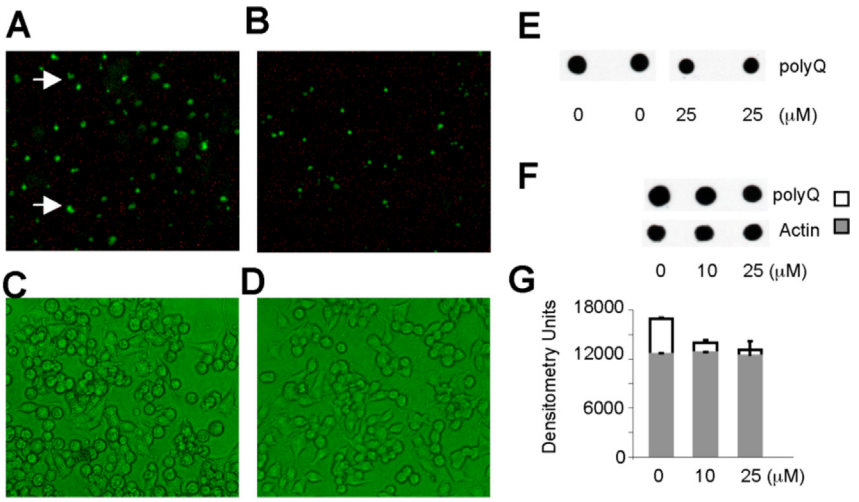

Fig. 4. Effects of SIRT2 inhibitors on polyglutamine aggregation in PC12 cells. **A-D**) Detection of aggregate inhibition using a microscopic epifluorescent assay. A) Aggregation of extended polyglutamine peptides containing HD103Q-EGFP in PC12 cells induced with 2.5 μM muristerone for 24 h, which results in the formation of punctuated fluorescent inclusions (indicated by arrows). B) Treatment with aggregation inhibitor(s) results in reduction of fluorescent inclusion number and size. C–D) Phase contrast cell images of (A) and (B) demonstrate equal cell density, i.e., lack of cytotoxicity. E–F) Polyglutamine aggregation dot-blot assay detects inhibition of polyglutamine aggregation with compounds **124** and **90**, respectively. G) Quantification of compound **90** inhibition of aggregation based on densitometry of immuno dot-blot (F). **90** reduces polyglutamine signal in a dose dependent manner but does not have an effect on actin (control).

[34,35], i.e., a dot-blot, assay. Albeit less sensitive than the epifluorescent method, the dot-blot assay provides a way to quantify the effect of treatment on aggregation (Fig. 4E). Five bioactive aggregation inhibitors were identified: compounds **64**, **90**, **124**, **126**, and **170**.

2.5. Chemical optimization and SAR

Because of low aqueous solubility (high lipophilicity) and metabolic instability, the initial stage of structural modification involved water solubility enhancement that would potentially improve the ADME properties. Lipinski's Rule of 5 [36] and Veber's rules [37] were adopted as the synthesis criteria, limiting the range for molecular weight to $\leq$ 500, calculated octanol–water partition coefficient (ClogP) to $\leq$5, the number of hydrogen bond donors (OH's and NH's) and hydrogen bond acceptors (N's and O's) to $\leq$10, the number of rotatable bonds $\leq$ 10, and the polar surface area $<$ 90 Å^2. The ideal ClogP value for BBB penetration, however, is $2 \leq \log P \leq 4$; therefore, most of the compounds that were synthesized were in that range. The syntheses are straightforward, mostly only 3–5 steps. Structures of the analogues were not determined at random; an initial structural hypothesis was proposed, which drove the synthetic effort. The synthesized compounds were tested for enhancement of solubility and activity, and the hypotheses were refined and adjusted according to the evolving results. The following structural modification strategies were applied to the **C2-8** and **AK-1** scaffolds to improve their solubility: (1) the A, B, and C phenyl rings (Fig. 1) of **C2-8** and **AK-1** were replaced with five- and six-membered heterocyclic ring(s), e.g., pyridine, pyrimidine, pyridazine, thiazole, oxazole, isoxazole, and oxadiazole rings. This is a common approach to increase aqueous solubility in drug design, for example, in the development of the HIV protease inhibitor, ritonavir [38]. Heterocyclic rings were found to be tolerated on ring A of **C2-8** but not on ring C, as described in the SAR section; (2) hydrophobic groups, halogens of **C2-8** and **AK-1**, were replaced with more polar and hydrophilic groups, such as hydroxyl, methoxyl, amino, cyano, carboxyl, acetyl, methylsulfoxide, methylsulfone, and acetamide groups. Four hydrophilic groups were found to increase, or at least maintain, the SIRT2 inhibitory activities: the cyano, sulfoxide, sulfone, and acetyl groups, specifically on ring A of **C2-8**; (3) the active derivatives from the above-mentioned strategies were combined into one compound. The structures of the new compounds are summarized along with their SIRT2 inhibitory activities at 10 μM in Tables S1–S3 (see Supporting Information).

An understanding of the SAR of the sulfobenzoic acid derivatives is not only important for the synthesis of more active analogues, but also crucial for selecting the optimum approaches for increasing solubility without significant loss in activity. Fig. 5 summarizes the SAR conclusions from the SIRT2 inhibition assays. Although **C2-8** and **AK-1** both contain a 3-sulfonyl benzoate scaffold, the SAR shows that their analogues have a few structurally distinct features, which differentiate the two scaffolds. On the basis of the SIRT2 inhibitory activities of analogues synthesized here and those tested in previous screening studies [4,5,21], the SAR of the **C2-8** scaffold can be summarized as follows: (1) R_1 on ring A of **C2-8** should be at the *para* position; however, small groups (e.g., F) at the *ortho* position are tolerated; (2) R_1 should be electron withdrawing, but both hydrophobic and hydrophilic substituents are tolerated; (3) Six-membered heterocyclic rings in place of benzene ring A are tolerated, but not five-membered heterocyclic rings; (4) The sulfonamide nitrogen must be methylated.; (5) R_3 is optimal at the *para* position; pyridinyl modification of ring C is tolerated; (6) R_3 should be electron withdrawing, and both hydrophobic and hydrophilic substituents are tolerated; (7) There is no apparent trend for R_2 on ring B; H, F, Cl, Br, CH_3, OCH_3 groups are tolerated at this position, and the replacement of this ring by a pyridine ring is also tolerated. (8) Inversion of the amide linkage will not improve activity; however, it will decrease selectivity for SIRT2 over SIRT1 and SIRT3, while a methylated amide linkage will retain the activity.

The SAR for the **AK-1** scaffold also has been studied and can be summarized as follows: (1) **AK-1** derivatives have optimum activities when R_1 is at the *meta* position, not *para*, which is favored for **C2-8** analogues; (2) R_1 should have electron-withdrawing or weakly electron-donating properties; (3) Similar to **C2-8**, both hydrophobic and hydrophilic substituents are tolerated at R_1; (4) Replacement of benzene ring A with five- and six-membered heterocyclic rings gives inactive compounds; (5) Hexamethyleneimine

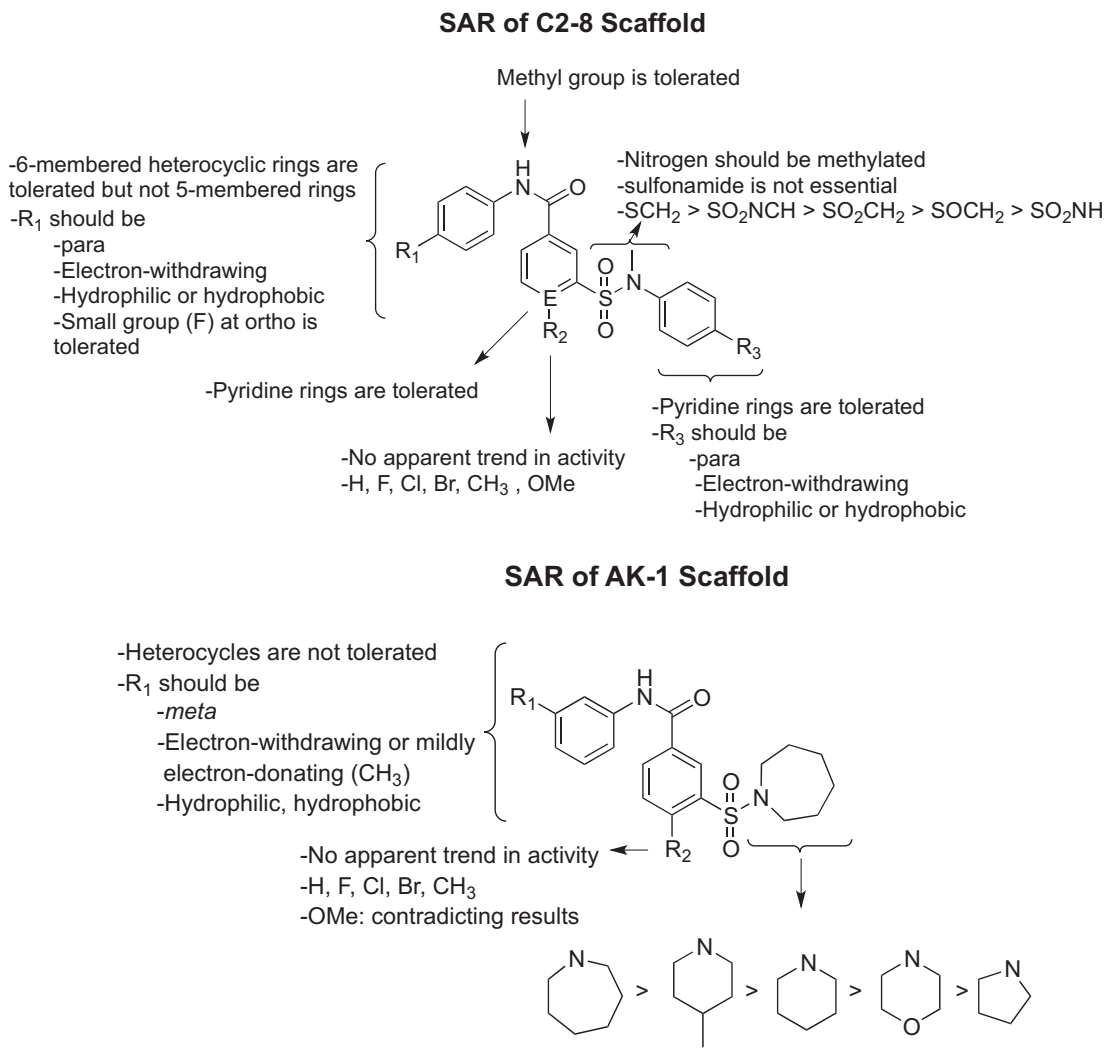

Fig. 5. Summary of SAR conclusions for the **C2-8** and **AK-1** scaffolds.

(seven-membered ring) is better than smaller cyclic ring amines. **AK-1** analogues that contain a 4-methylpiperidine group are more potent than those containing a piperidine group. These results suggest that ring C may be involved in a hydrophobic interaction in a binding pocket; (6) There is no apparent trend for R_2 on ring B; H, F, Cl, Br, CH_3 groups are tolerated at this position, and a OCH_3 group decreases SIRT2 inhibitory activity.

2.6. In vitro ADME profiling

Identified SIRT2 inhibitors were subjected to *in vitro* ADME assays, carried out at Apredica, Inc. (Watertown, MA). ADME profiling was conducted early in this study to evaluate the metabolic stability and pharmacokinetic behavior of the newly synthesized sulfobenzoic acid derivatives compared to **AK-1**. Two active analogues, **51** and **59**, were chosen for ADME profiling. The solubility of **51** and **59** in PBS was moderately increased by two- and four-fold, respectively, compared to **AK-1**. The plasma protein binding for both compounds is high: 99.8% for **51** and 99.1% for **59**. Microsomal stability is still low; neither compound was stable in mouse or human microsomes after 60 min (0% remaining for **51** and 16% for **59**). The efflux ratio is 0.7 and 1.7 for **51** and **59**, respectively, which suggests that they are not substrates for P-glycoprotein or other active transporters.

In an attempt to better understand the microsome instability of these compounds, **51** and **59** were submitted for metabolite identification studies at Apredica, Inc. The *N*-demethylated metabolite of **51** was detected, which we had already tested (**26**) and found to be inactive in the SIRT2 assay. This rapid metabolism of **51** to an inactive metabolite explains why this compound appears to have a low concentration in blood and in brain homogenate. Other active compounds became inactive when the *N*-methyl group was removed.

The major metabolite from **59** is the corresponding sulfone (**61**; the sulfoxide is oxidized to the sulfone). Unlike the loss in activity when the N–CH_3 group is demethylated, oxidation of the sulfoxide to the sulfone produces a more potent compound in both the SIRT2 and cell-based tubulin deacetylation assays. One of the most potent compounds in that series, however, is the corresponding nitrile (**64**), which avoids potential sulfur oxidation because there is no sulfoxide group. Compound **71**, a cyanopyridine analogue, is also more potent than **59**.

The other significant result from the metabolite identification study was that no amide hydrolysis products were detected in microsomal incubations, and limited hydrolysis was detected in

plasma (half-lives > 2 h). This supports the stability of the amide linkage.

As mentioned above, one of the few hydrophilic functional groups used to enhance solubility that was found to be active in SIRT2 inhibition is the acetyl group. However, it is well known that it is susceptible to reduction to the corresponding secondary alcohol by aldo-keto reductases [39]. To test if the secondary alcohol derivatives maintain SIRT2 inhibitory activity, acetyl analogues **103**, **104**, and **107** were reduced to their corresponding alcohols (**126**, **127**, and **128**). Compound **126** (SIRT2 $IC_{50} \sim 17$ μM) was found to have slightly better SIRT2 inhibitory activity than **103** (SIRT2 $IC_{50} \sim 25$ μM). The detailed results of *in vitro* ADME studies are given in the Supporting Information.

3. Conclusions

Starting with **C2-8** and **AK-1** as lead compounds, we have been able to alter their structures to enhance potency, water solubility, and metabolic stability. Synthesis of 176 compounds allowed the derivation of a SAR for these two classes of compounds. Fifteen compounds showed inhibitory activities greater than that of the reference compound (**AK-1**) with a threefold increase in potency. Active SIRT2 inhibitors were tested in a cell-based acetylation assay, and five of them increased α-tubulin acetylation in a dose-dependent manner in two neuronal cell lines, and eight of them increased acetylation in at least one of the two cell lines. Additionally, active SIRT2 inhibitors were tested in a tertiary aggregation assay, and five compounds were found to inhibit polyglutamine aggregation in PC12 cells. The best substituents on the aromatic ring are cyano, acetyl, 1-hydroxyethyl, methylthio. The results from this study are essential for further improvements of selective SIRT2 inhibitors.

4. Experimental section

4.1. General experimental procedures for compound synthesis

^{1}H NMR and ^{13}C NMR spectra were recorded on a Bruker Avance III (500 MHz ^{1}H, 125 MHz ^{13}C) with a DCH Cryo-Probe. Chemical shift values (δ) are reported in parts per million (ppm) relative to $CDCl_3$ [δ 7.26 ppm (1H), 77.16 ppm (13C)]. The proton spectra are reported as follows: δ (multiplicity, number of protons). Multiplicities are indicated by s (singlet), d (doublet), t (triplet), q (quartet), p (pentet), h (heptet), m (multiplet), and br (broad). The HREIMS experiments were conducted on a 6200-TOF LCMS (Agilent, Santa Clara, CA) equipped with a multimode source (mixed source that can ionize the samples alternatively by ESI or APCI). Electrospray mass spectra (ESMS) were obtained using an LCQ-Advantage with methanol as the solvent in the positive ion mode. Analytical HPLC analyses were performed on a Beckman HPLC system using a Vydac C18 column (4.6 × 150; 5 μm Phenomenex) and isocratic elution (CH_3CN:H_2O; 60:40) with UV detection set at 305 and 220 nm to verify the purity of tested compounds. Except for compounds **28**, **75**, and **147** a purity of >95% has been established for all final tested compounds. Compounds **28**, **75**, and **147** achieved 89%, 90%, and 88% purity levels, respectively. Except as otherwise indicated, all reactions were magnetically stirred and monitored by analytical thin-layer chromatography using Whatman precoated silica gel flexible plates (0.25 mm) with F254 indicator or Merck precoated silica gel plates with F254 indicator. Visualization was accomplished by UV light (256 nm). Flash column chromatography was performed using silica gel 60 (mesh 230–400) supplied by E. Merck. Yields refer to chromatographically and spectrographically pure compounds, unless otherwise noted. Commercial grade reagents and solvents were used without further purification except as indicated below.

4.2. General chemical reaction procedures

(A) **Chlorosulfonation of benzoic acid derivatives**. A mixture of **1** (5 g, 40.94 mmol) or **2** (5 g, 32.86 mmol) in chlorosulfonic acid (20 mL) was heated to 65 °C in an oil bath for 4 h, after which time TLC indicated complete conversion of the starting material to the intermediates, 3-(chlorosulfonyl)benzoic acid (**3**) and 3-(chlorosulfonyl)-4-methoxybenzoic acid (**4**), respectively. The reaction mixture was slowly poured over ice and filtered. The solid was dried in vacuo to yield intermediates **3** (7.90 g, 87%) and **4** (6.40 g, 86%), which were carried forward without further purification.

(B) **Formation of the sulfonamide bonds.** Sulfonyl chloride derivative **1** or **2** (3.99 mmol) was added gradually to a mixture of substituted amine (4.39 mmol) and pyridine (2 mL) in EtOAc with stirring at 0 °C. The reaction mixture was stirred at room temperature until the TLC indicated complete conversion of the sulfonyl chloride to the sulfonamide intermediate. The reaction mixture was dissolved in DCM and extracted (2×) with 10% NaOH. After the aqueous layer was acidified with 2 N HCl, the precipitate was collected by filtration, washed with H_2O, and dried in vacuo to give the desired products (**5**–**22**, **173**, **174**), which were carried forward without further purification.

(C) **Formation of the amide bond**. To a stirred solution of the amine (0.169 mmol), the carboxylic acid (**5**–**22**, 0.154 mmol), and with or without DMAP (0.154 mmol) in DCM (10 mL) at room temperature was added EDCI (0.308 mmol). The reaction mixture was stirred overnight and then concentrated in vacuo. The crude material was purified by flash chromatography (EtOAc/hexane) to afford the desired product (**23**–**152, 169, 170, 175, 176**).

(D) **Self-catalyzed selective oxidation of the methylthio aniline to the methylsulfinyl aniline**. Aminothioanisoles **153**, **154**, or **161** (1.0 g, 7.18 mmol) and H_2O_2 (0.74 mL, 30 wt% in H_2O, 7.18 mmol) were stirred at 70 °C for 1 h. The mixture was then cooled to room temperature and extracted with DCM (20 mL × 2). After drying with anhydrous Na_2SO_4, the organic solvent was removed in vacuo, and a brownish solid of the desired product (**155**, **156**, and **163**) was obtained.

(E) **Oxidation of methylthio aniline to methylsulfonyl aniline**. A mixture of Na_2WO_4 (0.067 g), 1 drop of acetic acid, and H_2O (5 mL) was placed in a flask and heated to 65 °C. Methylthio aniline **153**, **154**, or **161** (500 mg, 3.59 mmol) was added, followed by dropwise addition of H_2O_2 (1.1 mL, 10.77 mmol). The mixture was stirred at 65 °C for 1.5 h and, after cooling, 80 mL of 1 N HCl and 50 mL of DCM were added. The layers were separated, and the aqueous phase was washed with additional DCM. The aqueous phase was basified with 25% NaOH and extracted with DCM. The organic phase was washed with brine and dried over Na_2SO_4. The solvent was removed to give methylsulfonyl aniline derivatives **157**, **158** and **164**.

(F) ***N*-Methylation of aniline**. Copper (II) acetate (0.550 g, 3.03 mmol) was added to a solution of the aniline (1.22 mmol) and pyridine (0.34 mL, 4.24 mmol) in dioxane (15 mL). The mixture was stirred for 15 min, methyl boronic acid (0.181 g, 3.03 mmol) was added, and the reaction was refluxed until the aniline was totally consumed (TLC analysis, 1.5–18 h). The reaction mixture was allowed to reach room temp, filtered through Celite, and the solvent was

evaporated. The residue was purified by flash chromatography (0 → 50% EtOAc/hexanes) to afford the *N*-methylaniline.

(G) **Demethylation of anisole compounds**. To a 10-mL flask was added **29**, **55**, **69**, **83**, or **151** (0.089 mmol) and anhydrous DCM (2 mL). An argon atmosphere was established and maintained. This mixture was cooled in a Dry Ice/acetone bath and boron tribromide (1 M in DCM, 0.107 mmol) was added via syringe through a septum. After the mixture was stirred overnight at room temperature, it was poured into ice water and extracted with dichloromethane. The extract was dried ($MgSO_4$) and concentrated. The crude material was purified by flash chromatography (EtOAc/hexane) to afford the desired products (**35**, **58**, **70**, **84**, **152**).

(H) **Reduction of acetyl analogues to the secondary alcohol derivatives.** Sodium borohydride (0.50 mmol) was added to a stirred solution of **103**, **104**, or **107** (0.118 mmol) in anhydrous methanol (5 mL). After being stirred overnight, the reaction mixture was concentrated in vacuo, and the residue was dissolved in DCM (25 mL). The organic layer was subsequently washed with distilled water (2 × 20 mL), the organic extract dried over $MgSO_4$, and concentrated in vacuo to afford the respective secondary alcohol analogues (**126**, **127**, and **128**).

(I) **Hydrogenation of the nitro group**: To a solution of **171** or **172** (1 mmol) in MeOH (5 mL) and EtOAc (5 mL), Pd/C (10%) (106 mg, 0.1 mmol) was added, and the resulting mixture was stirred overnight under a H_2 gas atmosphere (1 atm) until the starting material was completely consumed. The product was filtered through Celite, concentrated, and purified by silica chromatography (EtOAc/hexanes) to afford the corresponding aniline (**173**, **174**).

4.2.1. *N-(4-cyanophenyl)-3-(N-(4-fluorophenyl)-N-methylsulfamoyl)benzamide (**47**)*

Compound **47** was prepared according to procedure C from 4-aminobenzonitrile (21.5 mg, 0.182 mmol) and **9** (50 mg, 0.162 mmol) to afford 39 mg of **46** (58%). ^{1}H NMR (500 MHz, $CDCl_3$) δ 3.17 (s, 3H), 6.99–7.05 (m, 4H), 7.61–7.83 (m, 4H), 7.81 (d, J = 8.8 Hz, 2H), 7.99 (s, 1H), 8.17 (dt, J = 1.6, 7.4 Hz, 1H), 8.27 (s, 1H). ^{13}C NMR (126 MHz, $CDCl_3$) δ 38.6, 107.9, 116.0, 116.2, 118.7, 120.2, 125.7, 128.6, 128.7, 129.9, 131.1, 132.4, 133.4, 135.2, 136.7, 136.8, 136.9, 141.6, 160.7, 162.7, 164.2. HRMS LC-TOF ($M + H^+$) calcd for $C_{21}H_{16}FN_3O_3S$ 410.0975, found 410.0969.

4.2.2. *3-(N-(4-chlorophenyl)-N-methylsulfamoyl)-N-(6-chloropyridazin-3-yl)benzamide (**51**)*

Compound **51** was prepared according to procedure C from 3-amino-6-chloropyridazine (37.6 mg, 0.29 mmol) and **10** (84.7 mg, 0.26 mmol) to afford 80.7 mg of **51** (71%). ^{1}H NMR (500 MHz, Acetone) δ 3.27 (s, 3H), 7.21 (d, J = 8.7 Hz, 2H), 7.38 (d, J = 8.7 Hz, 2H), 7.73 (dd, J = 1.2, 7.9 Hz, 1H), 7.78 (t, J = 7.8 Hz, 1H), 7.86 (d, J = 9.3 Hz, 1H), 8.37 (s, 1H), 8.45 (dd, J = 1.2, 7.9 Hz, 1H), 8.61 (d, J = 9.3 Hz, 1H). ^{13}C NMR (126 MHz, Acetone) δ 38.6, 122.8, 128.1, 129.0, 129.8, 130.5, 130.6, 132.2, 133.4, 133.4, 135.6, 138.0, 141.2, 153.0, 156.2, 166.0; HRMS LC-TOF ($M + H^+$) calcd for $C_{18}H_{14}Cl_2N_4O_3S$ 437.0242, found 437.0239.

4.2.3. *3-(N-(4-chlorophenyl)-N-methylsulfamoyl)-N-(5-fluoropyridin-2-yl)benzamide (**54**)*

Compound **54** was prepared according to procedure C to afford 50 mg of white powder (77%). ^{1}H NMR (500 MHz, $CDCl_3$) δ 3.17 (s, 3H), 7.02 (d, J = 8.9 Hz, 2H), 7.45 (d, J = 8.9 Hz, 2H), 7.50–54 (m, 1H), 7.59 (t, J = 7.9 Hz, 1H), 7.64 (d, J = 7.9 Hz, 1H), 8.06 (d, J = 3.0 Hz, 1H), 8.14–8.16 (m, 2H), 8.35 (dd, J = 4.1, 9.2 Hz, 1H), 9.08 (s, 1H). ^{13}C NMR (126 MHz, $CDCl_3$) δ 38.2, 115.3, 115.4, 125.4, 125.5, 126.4, 127.8, 127.8, 129.3, 129.6, 131.1, 131.9, 133.5, 135.1, 135.4, 135.6, 137.1, 139.6, 147.4, 147.4, 155.6, 157.6, 163.9. HRMS LCQ ($M + H^+$) 420.0577.

4.2.4. *3-(N-(4-chlorophenyl)-N-methylsulfamoyl)-N-(4-(methylsulfinyl)phenyl)benzamide (**59**)*

Compound **59** was prepared according to procedure C from 4-aminobenzonitrile (45.0 mg, 0.29 mmol) and **10** (84.7 mg, 0.26 mmol) to afford 109.5 mg of **59** (91%). ^{1}H NMR (500 MHz, $CDCl_3$) δ 2.74 (s, 3H), 3.20 (s, 3H), 7.04 (d, J = 8.8 Hz, 2H), 7.29 (d, J = 8.8 Hz, 2H), 7.58–7.64 (m, 4H), 7.85 (d, J = 7.0 Hz, 2H), 8.13 (s, 1H), 8.20 (d, J = 7.4 Hz, 1H), 9.23 (s, 1H). ^{13}C NMR (126 MHz, $CDCl_3$) δ 38.3, 43.7, 121.2, 121.3, 124.7, 126.1, 128.0, 129.3, 129.6, 130.8, 132.6, 133.6, 135.6, 136.7, 139.5, 140.3, 140.8, 164.6. HRMS LC-TOF ($M + H^+$) calcd for $C_{21}H_{19}ClN_2O_4S_2$ 463.0553, found 463.0544.

4.2.5. *3-(N-(4-chlorophenyl)-N-methylsulfamoyl)-N-(4-(methylsulfonyl)phenyl)benzamide (**61**)*

Compound **61** was prepared according to procedure C from 4-(methylsulfonyl)aniline (**157**, 29.0 mg, 0.169 mmol) and **10** (50 mg, 0.154 mmol) to afford 56.1 mg of **71** (76%). ^{1}H NMR (500 MHz, $CDCl_3$) δ 3.07 (s, 3H), 3.19 (s, 3H), 7.03 (d, J = 8.7 Hz, 2H), 7.30 (d, J = 8.7 Hz, 2H), 7.59–7.65 (m, 2H), 7.85 (d, J = 8.8 Hz, 2H), 7.89 (d, J = 8.8 Hz, 2H), 8.04 (s, 1H), 8.17 (d, J = 7.5 Hz, 1H), 8.42 (s, 1H). ^{13}C NMR (126 MHz, $CDCl_3$) δ 38.3, 44.6, 114.1, 120.4, 125.8, 128.0, 128.7, 129.3, 129.8, 131.1, 132.4, 133.6, 135.2, 135.8, 136.9, 139.4, 142.4, 164.3. HRMS LC-TOF ($M + H^+$) calcd for $C_{21}H_{19}ClN_2O_5S_2$ 479.0502, found 479.0497.

4.2.6. *3-(N-(4-chlorophenyl)-N-methylsulfamoyl)-N-(4-cyanophenyl)benzamide (**64**)*

Compound **64** was prepared according to procedure C from 4-aminobenzonitrile (20.0 mg, 0.169 mmol) and **10** (50 mg, 0.154 mmol) to afford 45.3 mg of **69** (76%). ^{1}H NMR (500 MHz, $CDCl_3$) δ 3.20 (s, 3H), 7.04 (d, J = 8.8 Hz, 2H), 7.30 (d, J = 8.9 Hz, 2H), 7.62–7.69 (m, 4H), 7.87 (dd, J = 1.9, 8.9 Hz, 2H), 8.08 (s, 1H), 8.21 (dt, J = 1.6, 7.4 Hz, 1H). ^{13}C NMR (126 MHz, $CDCl_3$) δ 42.2, 111.0, 122.8, 124.4, 130.3, 131.8, 131.9, 131.9, 133.2, 133.2, 133.3, 133.4, 134.8, 136.5, 137.1, 137.5, 139.5, 140.6, 143.4, 146.5, 169.1. HRMS LC-TOF ($M + H^+$) calcd for $C_{21}H_{16}ClN_3O_3S$ 426.0679, found 426.0673.

4.2.7. *3-(N-(4-chlorophenyl)-N-methylsulfamoyl)-N-(5-cyanopyridin-2-yl)benzamide (**71**)*

Compound **71** was prepared according to procedure C from 4′-aminoacetophenone (22.3 mg, 0.165 mmol) and **10** (50 mg, 0.154 mmol) to afford 33.5 mg of **71** (51%). ^{1}H NMR (500 MHz, $CDCl_3$) δ 3.20 (s, 3H), 7.05 (d, J = 8.8 Hz, 2H), 7.31 (d, J = 8.8 Hz, 2H), 7.67 (t, J = 7.8 Hz, 1H), 7.73 (dt, J = 1.3, 8.0 Hz, 1H), 8.03 (dd, J = 2.2, 8.7 Hz, 1H), 8.09 (t, J = 1.6 Hz, 1H), 8.18 (dt, J = 1.3, 8.0 Hz, 1H), 8.50 (d, J = 8.7 Hz, 1H), 8.62 (d, J = 1.7 Hz, 1H), 8.76 (s, 1H). ^{13}C NMR (126 MHz, $CDCl_3$) δ 38.3, 105.8, 113.9, 116.6, 126.2, 127.9, 129.4, 129.9, 131.6, 131.9, 133.7, 134.3, 137.4, 139.5, 141.9, 151.8, 153.5, 164.0. HRMS LC-TOF ($M + H^+$) calcd for $C_{20}H_{15}ClN_4O_3S$ 427.0632, found 427.0624.

4.2.8. *N-(4-cyanophenyl)-3-(N-(4-methoxyphenyl)-N-methylsulfamoyl)benzamide (**90**)*

Compound **90** was prepared according to procedure C from 4-aminobenzonitrile (20.2 mg, 0.171 mmol) and **12** (50 mg, 0.156 mmol) to afford 44.7 mg of **90** (68%). ^{1}H NMR (500 MHz, DMSO) δ 3.15 (s, 3H), 3.73 (s, 3H), 6.88 (d, J = 9.0 Hz, 2H), 7.0 (d, J = 9.0 Hz, 2H), 7.66 (dt, J = 1.2, 8.1 Hz, 1H), 7.76 (t, J = 7.8 Hz, 1H), 7.85 (d, J = 8.8 Hz, 2H), 7.97 (d, J = 8.8 Hz, 2H), 8.14 (t, J = 1.7 Hz, 1H), 8.27 (dt, J = 1.2, 8.0 Hz, 1H), 10.89 (brs, 1H). ^{13}C NMR (126 MHz,

DMSO) δ 38.4, 55.3, 105.7, 114.1, 119.0, 120.4, 126.7, 127.9, 129.6, 130.6, 132.4, 133.2, 133.3, 135.1, 136.5, 143.1, 158.3, 164.6. HRMS LC-TOF ($M + H^+$) calcd for $C_{22}H_{19}N_3O_4S$ 422.1175, found 422.1167.

4.2.9. 3-(N-(4-acetylphenyl)-N-methylsulfamoyl)-N-(4-chlorophenyl)benzamide (**102**)

Compound **102** was prepared according to procedure C from 4-chloroaniline (21.6 mg, 0.169 mmol) and **14** (50 mg, 0.150 mmol) to afford 59.1 mg of **102** (89%). ^{1}H NMR (500 MHz, $CDCl_3$) δ 2.57 (s, 3H), 3.20 (s, 3H), 7.19 (d, J = 8.7 Hz, 2H), 7.31 (d, J = 8.7 Hz, 2H), 7.56–7.60 (m, 4H), 7.88 (d, J = 8.6 Hz, 2H), 8.01 (s, 1H), 8.13 (dt, J = 1.9, 6.6 Hz, 1H), 8.27 (s, 1H). ^{13}C NMR (126 MHz, $CDCl_3$) δ 26.7, 37.9, 121.7, 125.6, 125.9, 129.1, 129.2, 129.7, 130.1, 130.5, 132.4, 135.6, 135.8, 136.0, 136.8, 145.1, 164.0, 197.1. HRMS LC-TOF ($M + H^+$) calcd for $C_{22}H_{19}ClN_2O_4S$ 443.0832, found 443.0826.

4.2.10. 3-(N-(4-acetylphenyl)-N-methylsulfamoyl)-N-(5-chloropyridin-2-yl)benzamide (**103**)

Compound **103** was prepared according to procedure C from 2-amino-5-chloropyridine (21.7 mg, 0.169 mmol) and **14** (50 mg, 0.150 mmol) to afford 45.8 mg of **103** (67%). ^{1}H NMR (500 MHz, $CDCl_3$) δ 2.61 (s, 3H), 3.25 (s, 3H), 7.25 (d, J = 8.7 Hz, 2H), 7.63 (t, J = 7.8 Hz, 1H), 7.71 (dt, J = 1.3, 8.0 Hz, 1H), 7.74 (dd, J = 2.6, 8.9 Hz, 1H), 7.94 (d, J = 8.7 Hz, 2H), 8.01 (t, J = 1.6 Hz, 1H), 8.15 (dt, J = 1.4, 7.9 Hz, 1H), 8.25 (d, J = 2.3 Hz, 1H), 8.31 (d, J = 8.9 Hz, 1H), 8.44 (brs, 1H). ^{13}C NMR (126 MHz, $CDCl_3$) δ 26.7, 37.9, 114.8, 125.8, 126.0, 127.5, 129.3, 129.8, 131.0, 131.9, 134.9, 135.7, 137.1, 138.2, 145.2, 146.7, 149.2, 163.6, 196.9. HRMS LC-TOF ($M + H^+$) calcd for $C_{21}H_{18}ClN_3O_4S$ 444.0785, found 444.0782.

4.2.11. 3-(N-(4-acetylphenyl)-N-methylsulfamoyl)-N-(4-cyanophenyl)benzamide (**106**)

Compound **106** was prepared according to procedure C from 4-aminobenzonitrile (20.2 mg, 0.169 mmol) and **14** (50 mg, 0.150 mmol) to afford 47.5 mg of **106** (73%). ^{1}H NMR (500 MHz, $CDCl_3$) δ 2.60 (s, 3H), 3.25 (s, 3H), 7.22 (d, J = 8.7 Hz, 2H), 7.61–7.69 (m, 4H), 7.80 (d, J = 8.8 Hz, 2H), 7.91 (d, J = 8.7 Hz, 2H), 8.02 (s, 1H), 8.16 (dt, J = 1.6, 7.4 Hz, 1H), 8.24 (s, 1H). ^{13}C NMR (126 MHz, $CDCl_3$) δ 26.7, 38.0, 108.0, 118.7, 120.2, 125.6, 126.0, 129.3, 130.0, 131.0, 132.5, 133.4, 135.3, 135.7, 137.1, 141.5, 145.1, 164.1, 197.1. HRMS LC-TOF ($M + H^+$) calcd for $C_{23}H_{19}N_3O_4S$ 434.1175, found 434.1169.

4.2.12. N-(4-acetylphenyl)-3-(N-(4-acetylphenyl)-N-methylsulfamoyl)benzamide (**109**)

Compound **109** was prepared according to procedure C from 6-amino-3-pyridinecarbonitrile (20.1 mg, 0.169 mmol) and **10** (50 mg, 0.154 mmol) to afford 60.8 mg of **109** (90%). ^{1}H NMR (500 MHz, $CDCl_3$) δ 2.48 (s, 3H), 2.49 (s, 3H), 3.15 (s, 3H), 7.14 (d, J = 7.1 Hz, 2H), 7.48–7.49 (m, 2H), 7.72 (d, J = 7.3 Hz, 2H), 7.80 (d, J = 7.1 Hz, 2H), 7.87 (d, J = 7.3 Hz, 2H), 8.08–8.10 (m, 2H). ^{13}C NMR (126 MHz, $CDCl_3$) δ 30.3, 30.5, 41.8, 123.8, 129.8, 130.5, 133.2, 133.4, 133.6, 134.4, 136.4, 136.8, 139.3, 139.8, 140.7, 146.8, 149.3, 169.1, 201.9, 202.1. HRMS LC-TOF ($M + H^+$) calcd for $C_{24}H_{22}N_2O_5S$ 451.1328, found 451.1327.

4.2.13. N-(4-cyanophenyl)-3-(N-methyl-N-(4-(methylsulfonyl)phenyl)sulfamoyl)benzamide (**115**)

Compound **115** was prepared according to procedure C from 4-aminobenzonitrile (16.0 mg, 0.149 mmol) and **16** (50 mg, 0.135 mmol) to afford 41.8 mg of **117** (66%). ^{1}H NMR (500 MHz, $CDCl_3$) δ 3.09 (s, 3H), 3.28 (s, 3H), 7.38 (d, J = 8.5 Hz, 2H), 7.64–7.68 (m, 4H), 7.88–7.92 (m, 4H), 8.17 (s, 1H), 8.21 (d, J = 6.9 Hz, 1H). ^{13}C NMR (126 MHz, $CDCl_3$) δ 37.8, 44.3, 107.2, 118.9, 120.4, 120.5, 126.4, 126.5, 128.4, 129.7, 130.5, 132.8, 133.2, 135.7, 136.6, 138.6, 142.4, 146.0, 164.8. HRMS LC-TOF ($M + H^+$) calcd for $C_{22}H_{19}N_3O_5S_2$ 470.0844, found 470.0840.

4.2.14. N-(4-chlorophenyl)-3-(N-methyl-N-(4-(methylsulfonyl)phenyl)sulfamoyl)benzamide (**117**)

Compound **117** was prepared according to procedure C from 6-chloroaniline (18.9 mg, 0.149 mmol) and **16** (50 mg, 0.135 mmol) to afford 56.9 mg of **117** (88%). ^{1}H NMR (500 MHz, $CDCl_3$) δ 3.08 (s, 3H), 3.26 (s, 3H), 7.33–7.37 (m, 4H), 7.60–7.65 (m, 4H), 7.89 (d, J = 8.8 Hz, 2H), 8.06 (s, 1H), 8.15 (dd, J = 1.6, 7.3 Hz, 1H). ^{13}C NMR (126 MHz, $CDCl_3$) δ 37.9, 44.4, 121.6, 121.7, 125.9, 126.5, 128.5, 129.2, 129.9, 130.1, 130.5, 132.4, 136.1, 136.8, 138.9, 146.0, 163.9. HRMS LC-TOF ($M + H^+$) calcd for $C_{21}H_{19}ClN_2O_5S_2$ 479.0502, found 479.0503.

4.2.15. 3-(N-(5-chloropyridin-2-yl)-N-methylsulfamoyl)-N-(4-cyanophenyl)benzamide (**124**)

Compound **124** was prepared according to procedure C to afford 46 mg of white powder (70%). ^{1}H NMR (500 MHz, $CDCl_3$) δ 3.25 (s, 3H), 7.57–7.62 (m, 2H), 7.67–7.71 (m, 4H), 7.82 (d, J = 8.8 Hz, 2H), 8.13–8.14 (m, 2H), 8.22 (dd, J = 0.5, 2.6 Hz, 1H), 8.36 (s, 1H). ^{13}C NMR (126 MHz, $CDCl_3$) δ 36.0, 107.8, 120.2, 121.7, 125.9, 129.8, 129.9, 130.9, 132.4, 133.4, 135.2, 137.7, 137.8, 141.6, 146.8, 151.5, 164.1. HRMS LCQ ($M + H^+$) 427.0550.

4.2.16. N-(4-cyanophenyl)-3-(N-(4-(1-hydroxyethyl)phenyl)-N-methylsulfamoyl)benzamide (**126**)

Compound **126** was prepared according to procedure K from **103** (25 mg, 0.058 mmol) to afford 23.1 mg of **126** (93%). ^{1}H NMR (500 MHz, $CDCl_3$) δ 1.46 (d, J = 6.3 Hz, 3H), 3.20 (s, 3H), 4.89 (q, J = 6.3 Hz, 1H), 7.05 (d, J = 8.5 Hz, 2H), 7.32 (d, J = 8.5 Hz, 2H), 7.64–7.68 (m, 3H), 7.75 (d, J = 7.9 Hz, 1H), 7.81 (d, J = 8.7 Hz, 2H), 7.93 (t, J = 1.5 Hz, 1H), 8.18 (d, J = 7.8 Hz, 1H), 8.24 (s, 1H). ^{13}C NMR (126 MHz, $CDCl_3$) δ 25.4, 38.4, 69.7, 107.9, 118.7, 120.2, 125.7, 126.2, 126.8, 129.8, 131.1, 132.4, 133.4, 135.0, 137.2, 140.0, 141.6, 145.6, 164.2. HRMS LC-TOF ($M + Na^+$) calcd for $C_{23}H_{21}N_3O_4S$ 458.1150, found 458.1141.

4.2.17. 3-(N-(4-bromophenyl)-N-methylsulfamoyl)-N-(4-chloro-2-fluorophenyl)-N-methylbenzamide (**165**)

Compound **165** was prepared according to procedure C from 4-chloro-2-fluoro-*N*-methylaniline (34.3 mg, 0.29 mmol) and **11** (80.8 mg, 0.26 mmol) to afford 89.6 mg of **165** as white solid (84%). ^{1}H NMR (500 MHz, CDCl3) δ 3.00 (s, 3H), 3.41 (s, 3H), 6.88 (d, J = 5.0 Hz 2H), 7.06 (m, 3H), 7.31 (m, 2H), 7.41 (d, J = 5.0 Hz, 1H), 7.43 (d, J = 5.0 Hz, 1H), 7.57 (s, 1H), 7.62 (s, 1H). ^{13}C NMR (126 MHz, CDCl3) δ 37.6, 37.9, 117.6 (d, J = 23.4 Hz), 121.2, 125.5 (d, J = 3.7 Hz), 127.1, 128.0, 128.8, 129.2, 130.0, 132.2, 132.3, 134.5 (d, J = 9.5 Hz), 136.1, 136.2, 140.1, 156.4 (d, J = 253.5 Hz), 169.5. HRMS (ESI) ($M + H^+$) calcd for $C_{21}H_{18}BrClFN_2O_3S$ 510.9894, found 510.9867.

4.2.18. N-(4-bromo-2-fluorophenyl)-3-(N-(4-bromophenyl)-N-methylsulfamoyl)-N-methylbenzamide (**166**)

Compound **166** was prepared according to procedure C from 4-bromo-2-fluoro-*N*-methylaniline (34.3 mg, 0.29 mmol) and **11** (80.8 mg, 0.26 mmol) to afford 89.6 mg of **166** as white solid (84%). ^{1}H NMR (500 MHz, $CDCl_3$) δ 3.0 (s, 3H), 3.40 (s, 3H), 6.88 (d, J = 8.2 Hz, 2H), 7.06–6.99 (t, J = 7.7 Hz, 1H), 7.22 (d, J = 8.3 Hz, 2H), 7.35–7.29 (m, 1H), 7.44–7.40 (m, 2H), 7.60–7.55 (m, 1H), 7.62 (s, 1H). ^{13}C NMR (126 MHz, $CDCl_3$) δ 37.5, 37.9, 120.5 (d, J = 23.1 Hz), 121.8 (d, J = 8.8 Hz), 127.0, 128.4 (d, J = 3.9 Hz), 128.8, 129.2, 130.3, 132.1, 132.3, 136.0, 136.2, 140.1, 156.9 (d, J = 254.7 Hz), 169.0. HRMS (ESI) $[M-Me]^-$ calcd for $C_{20}H_{14}Br_2FN_2O_3S$: 540.9055, found 540.9086.

4.2.19. 3-(N-(4-chlorophenyl)-N-methylsulfamoyl)-N-(4-cyano-2-fluorophenyl)benzamide (**167**)

Compound **167** was prepared according to procedure C from 4-amino-3-fluorobenzonitrile (34.3 mg, 0.29 mmol) and **10** (80.8 mg, 0.26 mmol) to afford 89.6 mg of **167** as white solid (84%). ^{1}H NMR (500 MHz, $CDCl_3$) δ 3.19 (s, 3H), 7.04 (dd, J = 8.6, 1.6 Hz, 2H), 7.29 (dd, J = 8.7, 1.6 Hz, 2H), 7.46 (dd, J = 10.4, 1.7 Hz, 1H), 7.53 (d, J = 8.6 Hz, 1H), 7.65 (t, J = 7.7 Hz, 1H), 7.70 (dd, J = 7.6, 1.7 Hz, 1H), 8.04–8.01 (m, 1H), 8.13 (dt, J = 7.5, 1.5 Hz, 1H), 8.30–8.25 (m, 1H), 8.60 (t, J = 8.1 Hz, 1H). ^{13}C NMR (126 MHz, $CDCl_3$) δ 38.1, 107.8 (d, J = 9.2 Hz), 117.6, 118.5 (d, J = 23.6 Hz), 118.9 (d, J = 21.9 Hz), 122.0, 122.3, 126.2, 128.1, 129.1, 129.6, 130.7 (d, J = 9.6 Hz), 131.9 (d, J = 15.2 Hz), 134.7, 137.3, 139.4, 151.6 (d, J = 247.4 Hz), 163.9. HRMS (ESI) $[M-H]^-$ calcd for $C_{21}H_{14}ClFN_3O_3S$: 442.0428, found 442.0450.

4.2.20. 2-(N-(4-chlorophenyl)-N-methylsulfamoyl)-N-(4-cyanophenyl)isonicotinamide (**169**)

Compound **169** was prepared according to procedure C from 4-aminobenzonitrile (95 mg, 0.8 mmol) and **168** (131 mg, 0.4 mmol) to afford 149 mg of **169** (87%). White solid; m.p. 195–197 °C; ^{1}H NMR (500 MHz, $CDCl_3$/DMSO-d6) δ 3.50 (s, 3H), 7.33–7.19 (m, 4H), 7.69–7.61 (m, 2H), 8.03–7.94 (m, 2H), 8.14 (s, 1H), 8.48 (s, 1H), 8.92 (s, 1H),10.82 (s, 1H). ^{13}C NMR (126 MHz, $CDCl_3$/DMSO-d6) δ 40.0, 107.1, 118.8, 120.6, 120.7, 125.6, 128.4, 129.1, 132.8, 133.0, 139.5, 142.4, 143.8, 150.6, 157.4, 162.9. HRMS (ESI) ($M + H^+$) calcd for $C_{20}H_{16}ClN_4O_3S$ 427.0632, found 427.0623.

4.2.21. 2-(N-(4-chlorophenyl)-N-methylsulfamoyl)-N-(4-cyano-2-fluorophenyl)isonicotinamide (**170**)

Compound **170** was prepared according to procedure B and C from **168** (321 mg, 1.0 mmol) to afford 361 mg of **170** as white solid (82%). White solid; m.p. 186–188 °C; ^{1}H NMR (500 MHz, $CDCl_3$) δ 3.51 (s, 3H), 7.18 (d, J = 8.8 Hz, 2H), 7.27 (m, 3H), 7.48 (dd, J = 10.3, 1.7 Hz, 1H), 7.55 (d, J = 8.6 Hz, 1H), 7.97 (dd, J = 4.9, 1.6 Hz, 1H), 8.11 (m, 1H), 8.28 (m, 1H), 8.59 (t, J = 8.1 Hz, 1H), 8.95 (d, J = 4.9 Hz, 1H). ^{13}C NMR (126 MHz, $CDCl_3$) δ 40.2, 108.6 (d, J = 9.3 Hz), 117.3 (d, J = 2.8 Hz), 118.8 (d, J = 22.7 Hz), 119.8, 122.2, 124.6, 128.4, 129.4, 129.6 (d, J = 3.7 Hz), 130.0 (d, J = 9.9 Hz), 133.6, 139.2, 142.8, 151.3, 151.6 (d, J = 246.2 Hz), 158.3, 162.1. HRMS (ESI) ($M + H^+$) calcd for $C_{20}H_{15}ClFN_4O_3S$ 445,0537, found 445.0544.

4.2.22. 4-Bromo-N-(3-(N-methyl-N-(4-(methylsulfonyl)phenyl) sulfamoyl)phenyl)benzamide (**175**)

Compound **175** was prepared according to procedure C from 4-bromobenzoic acid (100 mg, 0.5 mmol) and **173** (102 mg, 0.3 mmol) to afford 131 mg of **175** as white solid (83%); m.p. 216–218 °C; ^{1}H NMR (500 MHz, DMSO) δ 3.22 (s, 3H), 3.23 (s, 3H), 7.25 (d, J = 7.6 Hz, 1H), 7.47 (d, J = 8.7 Hz, 2H), 7.60–7.55 (m, 1H), 7.77 (d, J = 8.5 Hz, 2H), 7.91 (d, J = 9.7 Hz, 4H), 8.14–8.10 (m, 2H), 10.64 (s, 1H). ^{13}C NMR (126 MHz, DMSO) δ 37.5, 43.4, 118.4, 122.2, 124.5, 125.8, 125.9, 127.9, 129.8, 129.9, 131.5, 133.3, 136.1, 138.5, 139.8, 145.4, 164.9. HRMS (ESI) ($M + H^+$) calcd for $C_{21}H_{20}BrN_2O_5S_2$ 522.9997, found 522.9996.

4.2.23. N-(3-(N-(4-chlorophenyl)-N-methylsulfamoyl)phenyl)-4-cyanobenzamide (**176**)

Compound **176** was prepared according to procedure C from 4-cyanobenzoic acid (147 mg, 1.0 mmol) and **174** (269 mg, 0.9 mmol) to afford 297 mg of **176** as white solid (78%). m.p. 196–198 °C; ^{1}H NMR (500 MHz, $CDCl_3$) δ 3.13 (s, 3H), 6.97 (d, J = 8.6 Hz, 2H), 7.24 (d, J = 10.5 Hz, 2H), 7.29 (d, J = 8.1 Hz, 1H), 7.53 (t, J = 8.0 Hz, 1H), 7.69 (s, 1H), 7.83 (d, J = 8.3 Hz, 2H), 8.08 (d, J = 8.3 Hz, 2H), 8.35 (d, J = 8.2 Hz, 1H), 8.60 (s, 1H). ^{13}C NMR (126 MHz, $CDCl_3$) δ 38.3, 115.7, 117.9, 119.0, 123.7, 124.9, 128.0, 128.1, 129.6, 130.1, 132.7, 133.6, 136.4, 137.9, 138.6, 139.5, 164.3. HRMS (ESI) ($M + H^+$) calcd for $C_{21}H_{16}ClN_3NaO_3S$ 448.0499, found 448.0500.

5. Experimental procedures for compound testing

5.1. Compound handling and storage

Newly synthesized compounds were dissolved in molecular biology grade dimethyl sulfoxide (DMSO) to a 10 mM stock concentration. Compound solutions were aliquoted and stored at −80 °C.

5.2. Testing of compounds in in vitro enzymatic assays

Modulation of sirtuins 1–3 activities by compounds was assessed using the Flour-de-Lys fluorescent biochemical assays available through Enzo Life Sciences, in 96-well format, as previously described [4]. Compounds were initially tested at the single dose of 10 μM in triplicate, with **AK-1** as reference compound. Identified SIRT2 inhibitors were retested in the same assay at multiple doses to determine SIRT2 IC_{50} values. They were also tested at multiple doses against SIRT1 and SIRT3 to determine their selectivity.

5.3. α-Tubulin acetylation assay

Compound bioactivity was tested in the rat embryonic striatal cell line, ST14A (a generous gift of E. Cattaneo) [40], and in the mouse Neuro2a (ATCC) cells. Cycling cells were treated with compounds up to 50 μM concentration for 6 h and then harvested with lysis buffer containing 2% SDS and protease inhibitors. Trichostatin A at 1 μM concentration was used as a positive control. Protein concentrations were evaluated using a BCA analysis kit (Thermo Scientific) and normalized. Samples were prepared in a SDS buffer containing DTT (New England Biolabs), separated on a 10% bis-acrylamide protein gel via electrophoresis, and transferred onto a 0.2 μm PVDF membrane (Bio-Rad). Membranes were probed for total α-tubulin (Sigma T6074, 1:10,000), acetylated α-tubulin (Sigma T6793, 1:2000) or GAPDH (Millipore MAB374, 1:10,000) overnight in 5% milk in PBST at 4 °C on a rocker. Membranes were thrice washed in PBST for 15 min on a shaker and incubated in an anti-mouse-HRP (Sigma A3682, 1:4000) secondary solution in 3% milk in PBST for 1.5 h at room temperature on a rocker. After four washes of 15 min in PBST on a shaker, blots were visualized using SuperSignal West Pico Chemiluminescent Substrate (Thermo Scientific) and exposed on scientific imaging films. A densiometric analysis of the blots was conducted using ImageJ software available from the National Institutes of Health, USA. Blot intensities were normalized to total α-tubulin or GAPDH.

5.4. Aggregation assay

Rat neuronal PC12 cells expressing HD103Q-EGFP fusion fragment of mutant huntingtin in inducible fashion [32,33] were treated simultaneously with compounds and 2.5 μM of ecdysone-**inducible** gene inducer muristerone A for a minimum of 24 h. **C2-8** was used as the reference compound in each experiment. Modulation of aggregation was assessed first visually by fluorescence microscopy and later by analysis of the aggregates using Western dot-blot. Cells were harvested with RIPA buffer containing protease inhibitors and centrifuged at 13,500 rpm for 15 min at 4 °C. Pellets were redissolved in lysis buffer containing 2% SDS and protease inhibitors with several cycles of sonication and boiling. Protein concentrations were evaluated using a BCA analysis kit (Thermo Scientific) and normalized. Samples were prepared in a SDS buffer

containing DTT (New England Biolabs) and spotted onto a 0.2 μm supported nitrocellulose membrane (Bio-Rad). Membranes were probed for actin (Sigma A2066, 1:1000), or polyQ (Millipore MAB1574, 1:4000) overnight in 5% milk in PBST at 4 °C on a rocker. Membranes were thrice washed in PBST for 15 min on a shaker and incubated in either an anti-mouse-HRP or anti-rabbit-HRP secondary solution in 3% milk in PBST for 1.5 h at room temperature on a rocker. After four washes of 15 min in PBST on a shaker, blots were visualized using SuperSignal West Dura Extended Duration Substrate (Thermo Scientific) and exposed on scientific imaging films. A densiometric analysis of the blots was conducted using ImageJ software available from the National Institutes of Health, USA. Blot intensities were normalized to actin.

Acknowledgments

The authors are grateful to the National Institutes of Health (Grant U01 NS066912) for financial support of this research.

Appendix A. Supplementary data

Supplementary data related to this article can be found at http://dx.doi.org/10.1016/j.ejmech.2014.02.003.

References

[1] (a) A. Raghavan, Z.A. Shah, Sirtuins in neurodegenerative diseases: a biological-chemical perspective, Neurodegenerative Disease 9 (2012) 1–10; (b) J. Schemies, U. Uciechowska, W. Sippl, M. Jung, NAD(+) -dependent histone deacetylases (sirtuins) as novel therapeutic targets, Medicinal Research Reviews 30 (2010) 861–889.

[2] B.J. North, B.L. Marshall, M.T. Borra, J.M. Denu, E. Verdin, The human Sir2 ortholog, SIRT2, is an NAD+-dependent tubulin deacetylase, Molecular Cell 11 (2003) 437–444.

[3] D.M. Taylor, M.M. Maxwell, R. Luthi-Carter, A.G. Kazantsev, Biological and potential therapeutic roles of sirtuin deacetylases, Cellular and Molecular Life Sciences 65 (2008) 4000–4018.

[4] T.F. Outeiro, E. Kontopoulos, S.M. Altmann, I. Kufareva, K.E. Strathearn, A.M. Amore, C.B. Volk, M.M. Maxwell, J.C. Rochet, P.J. McLean, A.B. Young, R. Abagyan, M.B. Feany, B.T. Hyman, A.G. Kazantsev, Sirtuin 2 inhibitors rescue alpha-synuclein-mediated toxicity in models of Parkinson's disease, Science 317 (2007) 516–519.

[5] R. Luthi-Carter, D.M. Taylor, J. Pallos, E. Lambert, A. Amore, A. Parker, H. Moffitt, D.L. Smith, H. Runne, O. Gokce, A. Kuhn, Z. Xiang, M.M. Maxwell, S.A. Reeves, G.P. Bates, C. Neri, L.M. Thompson, J.L. Marsh, A.G. Kazantsev, SIRT2 inhibition achieves neuroprotection by decreasing sterol biosynthesis, Proceedings of the National Academy of Sciences 107 (2010) 7927–7932.

[6] Y.H. Jin, Y.J. Kim, D.W. Kim, K.H. Baek, B.Y. Kang, C.Y. Yeo, K.Y. Lee, Sirt2 interacts with 14–3-3 beta/gamma and downregulates the activity of p53, Biochemical and Biophysical Research Communications 368 (2008) 690–695.

[7] M. Hiratsuka, T. Inoue, T. Toda, N. Kimura, Y. Shirayoshi, H. Kamitani, T. Watanabe, E. Ohama, C.G. Tahimic, A. Kurimasa, M. Oshimura, Proteomics-based identification of differentially expressed genes in human gliomas: down-regulation of SIRT2 gene, Biochemical and Biophysical Research Communications 309 (2003) 558–566.

[8] B.J. North, E. Verdin, Mitotic regulation of SIRT2 by cyclin-dependent kinase 1-dependent phosphorylation, The Journal of Biological Chemistry 282 (2007) 19546–19555.

[9] T. Inoue, Y. Nakayama, H. Yamada, Y.C. Li, S. Yamaguchi, M. Osaki, A. Kurimasa, M. Hiratsuka, M. Katoh, M. Oshimura, SIRT2 downregulation confers resistance to microtubule inhibitors by prolonging chronic mitotic arrest, Cell Cycle 8 (2009) 1279–1291.

[10] M.S. Christodoulou, A. Sacchetti, V. Ronchetti, S. Caufin, A. Silvani, G. Lesma, G. Fontana, F. Minicone, B. Riva, M. Ventura, M. Lahtela-Kakkonen, E. Jarho, V. Zuco, F. Zunino, N. Martinet, F. Dapiaggi, S. Pieraccini, M. Sironi, L. Dalla Via, O.M. Gia, D. Passarella, Quinazolinecarboline alkaloid evodiamine as scaffold for targeting topoisomerase I and sirtuins, Bioorganic & Medicinal Chemistry 21 (2013) 6920–6928.

[11] P. Mellini, T. Kokkola, T. Suuronen, H.S. Salo, L. Tolvanen, A. Mai, M. Lahtela-Kakkonen, E.M. Jarho, Screen of pseudopeptidic inhibitors of human sirtuins 1-3: two lead compounds with antiproliferative effects in cancer cells, Journal of Medicinal Chemistry 56 (2013) 6681–6695.

[12] A. Nakhi, P.T. Srinivas, M.S. Rahman, R. Kishore, G.P. Seerapu, K. Lalith Kumar, D. Haldar, M.V. Rao, M. Pal, Amberlite IR-120H catalyzed MCR: design, synthesis and crystal structure analysis of 1,8-dioxodecahydroacridines as potential inhibitors of sirtuins, Bioorganic & Medicinal Chemistry Letters 23 (2013) 1828–1833.

[13] J.S. Disch, G. Evindar, C.H. Chiu, C.A. Blum, H. Dai, L. Jin, E. Schuman, K.E. Lind, S.L. Belyanskaya, J. Deng, F. Coppo, L. Aquilani, T.L. Graybill, J.W. Cuozzo, S. Lavu, C. Mao, G.P. Vlasuk, R.B. Perni, Discovery of thieno[3,2-d]pyrimidine-6-carboxamides as potent inhibitors of SIRT1, SIRT2, and SIRT3, Journal of Medicinal Chemistry 56 (2013) 3666–3679.

[14] D. Rotili, D. Tarantino, A. Nebbioso, C. Paolini, C. Huidobro, E. Lara, P. Mellini, A. Lenoci, R. Pezzi, G. Botta, M. Lahtela-Kakkonen, A. Poso, C. Steinkuhler, P. Gallinari, R. De Maria, M. Fraga, M. Esteller, L. Altucci, A. Mai, Discovery of salermide-related sirtuin inhibitors: binding mode studies and antiproliferative effects in cancer cells including cancer stem cells, Journal of Medicinal Chemistry 55 (2012) 10937–10947.

[15] P. Mellini, V. Carafa, B. Di Rienzo, D. Rotili, D. De Vita, R. Cirilli, B. Gallinella, D.P. Provvisiero, S. Di Maro, E. Novellino, L. Altucci, A. Mai, Carprofen analogues as sirtuin inhibitors: enzyme and cellular studies, ChemMedChem 7 (2012) 1905–1908.

[16] D. Rotili, D. Tarantino, V. Carafa, C. Paolini, J. Schemies, M. Jung, G. Botta, S. Di Maro, E. Novellino, C. Steinkuhler, R. De Maria, P. Gallinari, L. Altucci, A. Mai, Benzodeazaoxaflavins as sirtuin inhibitors with antiproliferative properties in cancer stem cells, Journal of Medicinal Chemistry 55 (2012) 8193–8197.

[17] M. Friden-Saxin, T. Seifert, M.R. Landergren, T. Suuronen, M. Lahtela-Kakkonen, E.M. Jarho, K. Luthman, Synthesis and evaluation of substituted chroman-4-one and chromone derivatives as sirtuin 2-selective inhibitors, Journal of Medicinal Chemistry 55 (2012) 7104–7113.

[18] T. Suzuki, M.N. Khan, H. Sawada, E. Imai, Y. Itoh, K. Yamatsuta, N. Tokuda, J. Takeuchi, T. Seko, H. Nakagawa, N. Miyata, Design, synthesis, and biological activity of a novel series of human sirtuin-2-selective inhibitors, Journal of Medicinal Chemistry 55 (2012) 5760–5773.

[19] M. Freitag, J. Schemies, T. Larsen, K. El Gaghlab, F. Schulz, T. Rumpf, M. Jung, A. Link, Synthesis and biological activity of splitomicin analogs targeted at human NAD(+)-dependent histone deacetylases (sirtuins), Bioorganic & Medicinal Chemistry 19 (2011) 3669–3677.

[20] T. Huhtiniemi, T. Suuronen, V.M. Rinne, C. Wittekindt, M. Lahtela-Kakkonen, E. Jarho, E.A. Wallen, A. Salminen, A. Poso, J. Leppanen, Oxadiazole-carbonylaminothioureas as SIRT1 and SIRT2 inhibitors, Journal of Medicinal Chemistry 51 (2008) 4377–4380.

[21] D.M. Taylor, U. Balabadra, Z. Xiang, B. Woodman, S. Meade, A. Amore, M.M. Maxwell, S. Reeves, G.P. Bates, R. Luthi-Carter, P.A. Lowden, A.G. Kazantsev, A brain-permeable small molecule reduces neuronal cholesterol by inhibiting activity of sirtuin 2 deacetylase, ACS Chemical Biology 6 (2011) 540–546.

[22] V. Chopra, L. Quinti, J. Kim, L. Vollor, K.L. Narayanan, C. Edgerly, P.M. Cipicchio, M.A. Lauver, S.H. Choi, R.B. Silverman, R.J. Ferrante, S. Hersch, A.G. Kazantsev, The sirtuin 2 inhibitor AK-7 is neuroprotective in Huntington's disease mouse models, Cell Reports 2 (2012) 1492–1497.

[23] X. Zhang, D.L. Smith, A.B. Meriin, S. Engemann, D.E. Russel, M. Roark, S.L. Washington, M.M. Maxwell, J.L. Marsh, L.M. Thompson, E.E. Wanker, A.B. Young, D.E. Housman, G.P. Bates, M.Y. Sherman, A.G. Kazantsev, A potent small molecule inhibits polyglutamine aggregation in Huntington's disease neurons and suppresses neurodegeneration in vivo, Proceedings of the National Academy of Sciences 102 (2005) 892–897.

[24] V. Chopra, J.H. Fox, G. Lieberman, K. Dorsey, W. Matson, P. Waldmeier, D.E. Housman, A. Kazantsev, A.B. Young, S. Hersch, A small-molecule therapeutic lead for Huntington's disease: preclinical pharmacology and efficacy of C2-8 in the R6/2 transgenic mouse, Proceedings of the National Academy of Sciences 104 (2007) 16685–16689.

[25] (a) Z. Nie, C. Perretta, J. Lu, Y. Su, S. Margosiak, K.S. Gajiwala, J. Cortez, V. Nikulin, K.M. Yager, K. Appelt, S. Chu, Structure-based design, synthesis, and study of potent inhibitors of beta-ketoacyl-acyl carrier protein synthase III as potential antimicrobial agents, Journal of Medicinal Chemistry 48 (2005) 1596–1609;
(b) J. Wrobel, D. Green, J. Jetter, W. Kao, J. Rogers, M.C. Perez, J. Hardenburg, D.C. Deecher, F.J. Lopez, B.J. Arey, E.S. Shen, Synthesis of (bis)sulfonic acid, (bis) benzamides as follicle-stimulating hormone (FSH) antagonists, Bioorganic & Medicinal Chemistry 10 (2002) 639–656.

[26] M. Beller, F. Shi, M.K. Tse, H.M. Kaiser, Self-catalyzed oxidation of sulfides with hydrogen peroxide: a green and practical process for the synthesis of sulfoxides, Advanced Synthesis & Catalysis 349 (2007) 2425–2430.

[27] M. Biava, G.C. Porretta, G. Poce, S. Supino, S. Forli, M. Rovini, A. Cappelli, F. Manetti, M. Botta, L. Sautebin, A. Rossi, C. Pergola, C. Ghelardini, E. Vivoli, F. Makovec, P. Anzellotti, P. Patrignani, M. Anzini, Cyclooxygenase-2 inhibitors. 1,5-diarylpyrrol-3-acetic esters with enhanced inhibitory activity toward cyclooxygenase-2 and improved cyclooxygenase-2/cyclooxygenase-1 selectivity, Journal of Medicinal Chemistry 50 (2007) 5403–5411.

[28] I. Gonzalez, J. Mosquera, C. Guerrero, R. Rodriguez, J. Cruces, Selective monomethylation of anilines by Cu(OAc)2-promoted cross-coupling with $MeB(OH)_2$, Organic Letters 11 (2009) 1677–1680.

[29] J.F.W. McOmie, D.E. West, 3,3'-dihydroxybiphenyl, Organic Syntheses, Coll 5 (1973) 412.

[30] P. Watts, C. Wiles, S.J. Haswell, Clean and selective oxidation of aromatic alcohols using silica-supported Jones' reagent in a pressure-driven flow reactor, Tetrahedron Letters 47 (2006) 5261–5264.

[31] H.H. Fox, J.T. Gibas, Nuclear substitution derivatives of isonicotinic acid, The Journal of Organic Chemistry 23 (1958) 64–66.

[32] A. Kazantsev, E. Preisinger, A. Dranovsky, D. Goldgaber, D. Housman, Insoluble detergent-resistant aggregates form between pathological and

nonpathological lengths of polyglutamine in mammalian cells, Proceedings of the National Academy of Sciences 96 (1999) 11404–11409.
[33] B.L. Apostol, A. Kazantsev, S. Raffioni, K. Illes, J. Pallos, L. Bodai, N. Slepko, J.E. Bear, F.B. Gertler, S. Hersch, D.E. Housman, J.L. Marsh, L.M. Thompson, A cell-based assay for aggregation inhibitors as therapeutics of polyglutamine-repeat disease and validation in drosophila, Proceedings of the National Academy of Sciences 100 (2003) 5950–5955.
[34] V. Heiser, E. Scherzinger, A. Boeddrich, E. Nordhoff, R. Lurz, N. Schugardt, H. Lehrach, E.E. Wanker, Inhibition of huntingtin fibrillogenesis by specific antibodies and small molecules: implications for Huntington's disease therapy, Proceedings of the National Academy of Sciences 97 (2000) 6739–6744.
[35] V. Heiser, S. Engemann, W. Brocker, I. Dunkel, A. Boeddrich, S. Waelter, E. Nordhoff, R. Lurz, N. Schugardt, S. Rautenberg, C. Herhaus, G. Barnickel, H. Bottcher, H. Lehrach, E.E. Wanker, Identification of benzothiazoles as potential polyglutamine aggregation inhibitors of Huntington's disease by using an automated filter retardation assay, Proceedings of the National Academy of Sciences 99 (Suppl. 4) (2002) 16400–16406.
[36] C.A. Lipinski, F. Lombardo, B.W. Dominy, P.J. Feeney, Experimental and computational approaches to estimate solubility and permeability in drug discovery and development settings, Advanced Drug Delivery Reviews 46 (2001) 3–26.
[37] D.F. Veber, S.R. Johnson, H.Y. Cheng, B.R. Smith, K.W. Ward, K.D. Kopple, Molecular properties that influence the oral bioavailability of drug candidates, Journal of Medicinal Chemistry 45 (2002) 2615–2623.
[38] D.J. Kempf, L. Codacovi, X.C. Wang, W.E. Kohlbrenner, N.E. Wideburg, A. Saldivar, S. Vasavanonda, K.C. Marsh, P. Bryant, H.L. Sham, et al., Symmetry-based inhibitors of HIV protease. Structure-activity studies of acylated 2,4-diamino-1,5-diphenyl-3-hydroxypentane and 2,5-diamino-1,6-diphenylhexane-3,4-diol, Journal of Medicinal Chemistry 36 (1993) 320–330.
[39] O.A. Barski, S.M. Tipparaju, A. Bhatnagar, The aldo-keto reductase superfamily and its role in drug metabolism and detoxification, Drug Metabolism Reviews 40 (2008) 553–624.
[40] M.E. Ehrlich, L. Conti, M. Toselli, L. Taglietti, E. Fiorillo, V. Taglietti, S. Ivkovic, B. Guinea, A. Tranberg, S. Sipione, D. Rigamonti, E. Cattaneo, ST14A cells have properties of a medium-size spiny neuron, Experimental Neurology 167 (2001) 215–226.